

Single-Crystalline GdB₆ Nanowire Field Emitters

Han Zhang,[†] Qi Zhang,[‡] Gongpu Zhao,[‡] Jie Tang,^{‡,§} Otto Zhou,^{†,‡} and Lu-Chang Qin^{*,†,‡}
Curriculum in Applied and Materials Sciences, Department of Physics and Astronomy, University of North Carolina at Chapel Hill, Chapel Hill, North Carolina 27599-3255, and National Institute for Materials Science, Tsukuba, Japan

Received June 28, 2005; E-mail: lcqin@physics.unc.edu

Rare-earth hexaborides are the best thermionic electron sources due to their low work function, low volatility at high temperature, high conductivity, high chemical resistance, and high mechanical strength.¹ Single-crystalline LaB₆ and CeB₆ (with work functions of about 2.5 eV) have shown this advantage in thermionic electron emission applications during the past 50 years. In the rare-earth hexaboride family, GdB₆ is believed to have the lowest work function (~1.5 eV).² However, satisfactory thermionic emission has not been achieved with this material, likely due to the relatively poor stability of GdB₆ at high working temperature around 1500 °C.^{2–4} Nevertheless, GdB₆'s extremely low work function offers a great opportunity for making this material room temperature field emitters that put less stringency on the high-temperature stability. A field emission electron source offers a brightness more than 100 times higher than the conventional thermionic electron sources, and its current density J can be expressed by the Fowler–Nordheim equation (in SI units):^{5,6}

$$J = 2.23 \times 10^{-25} (E^2/\phi) \exp(4.12 \times 10^{-9}/\phi^{1/2} - 1.02 \times 10^{38} \phi^{3/2}/E) \text{ A/m}^2$$

where E is the local field produced at the tip, and ϕ is the work function of the emitting surface of the tip. It can be inferred that the emission current density J increases rapidly with an increasing electric field E , which can be expressed as $E = \beta V$, with V being the voltage applied on the emitter tip and β a geometry-dependent enhancement factor that becomes larger as the emitter tip is sharper. It can also be seen that the emission current density J is enhanced almost exponentially with the decrease of work function, ϕ . A recent study also indicates that, in electron optical applications, reducing the emitter's work function is the only way to achieve high brightness without increasing the electron energy spread, which causes chromatic aberrations.⁶ Therefore, to obtain a high emission current with small energy spread at a convenient working voltage, sharp field emitters out of low work function materials, for example, rare-earth hexaboride nanowires, are desired. In our previous work, we have demonstrated the synthesis of $\langle 111 \rangle$ oriented LaB₆ nanowires, $\langle 001 \rangle$ oriented LaB₆ nanowires, and $\langle 001 \rangle$ oriented CeB₆ nanowires and also demonstrated field emission from a single LaB₆ nanowire emitter with a current density as high as 5×10^5 A/cm² at a working voltage of 800 V.^{7–9} In this communication, we present for the first time a successful synthesis of single-crystalline GdB₆ nanowires and a measurement of their field electron emission.

The synthesis is based on the following chemical reaction:



The reaction was conducted in a similar chemical vapor deposition

(CVD) system described before,⁷ except that GdCl₃ powders (99.99%, Aldrich) were used as the evaporation source and a clean silicon wafer was used as the deposition substrate.

After the reaction, a scanning electron microscope (SEM, JEM-6300) equipped with an energy-dispersive X-ray spectrometer (EDX, KeveX Sigma3) was used to examine the nanowires. The lateral dimensions of the nanowires range from below 100 nm to more than 1 μm. EDX analysis indicates the nanowires are composed of B and Gd elements.

The GdB₆ nanowires were also examined in a transmission electron microscope (TEM, JEM-2010F) operated at 200 kV. Figure 1a is a morphological image of the grown GdB₆ nanowires. They are typically 50–60 nm in lateral dimensions and are more than several microns in length. The nanowires' tip-top surfaces are flat and form a right angle with the side surfaces, as can be clearly seen in the inserted high-resolution image of the area marked by an arrow. The nanowires were found to grow along their $\langle 001 \rangle$ lattice directions, and both the tip-top and the side surfaces are terminated with the $\{100\}$ lattice planes. Panels b and c of Figure 1 are the TEM images together with their corresponding selected area electron diffraction patterns taken from a single GdB₆ nanowire along its $[100]$ and $[2\bar{1}0]$ lattice directions, respectively. A simple geometric calculation was performed, as illustrated in Figure 1d, in order to obtain the morphology of the nanowire tip. By using $B = 56$ nm measured from Figure 1b, $C = 68$ nm from Figure 1c, and $\theta = 26.6^\circ$ determined from the two diffraction patterns, we obtained the nanowire's other side length A from the equation $A = (C - B \cos \theta)/\sin \theta = 40$ nm.

To study its field emission properties, a GdB₆ nanowire with lateral dimension of about 200 nm was picked up under an optical microscope assisted with a manipulator, and the nanowire was then attached onto an etched 0.5 mm tungsten (W) tip with an acrylic adhesive. Field emission was measured in a high vacuum chamber of 10^{-7} Torr. With the W tip as the cathode and a phosphor-coated ITO glass as the anode spaced at 250 μm, an increasing electric voltage was then applied and, in the meantime, the emission current was measured and the emission patterns were recorded with a CCD camera simultaneously.

Figure 2a shows the I – V curve of the field emission from the GdB₆ single nanowire. An emission current of 10 nA was obtained at a voltage of 650 V, and the emission current reached 200 nA before the emitter broke down. During the entire emission process, the emitter's surface is estimated to reach a maximum temperature of about 400 °C, which is much lower than the melting point (2510 °C) of GdB₆, but is much higher than the acrylic adhesive's tolerance temperature of 60 °C. The large current fluctuations observed in the I – V curve are therefore suggested to be caused by the melting of the adhesive attaching the GdB₆ nanowire to the W tip. A Fowler–Nordheim plot ($\ln(I/V^2)$ vs $1/V$) is depicted in Figure 2b, revealing characteristics of metallic field emission. Figure 2c is a low-magnification TEM image of the GdB₆ nanowire emitter,

[†] Curriculum in Applied and Materials Sciences, University of North Carolina.

[‡] Department of Physics and Astronomy, University of North Carolina.

[§] National Institute for Materials Science.

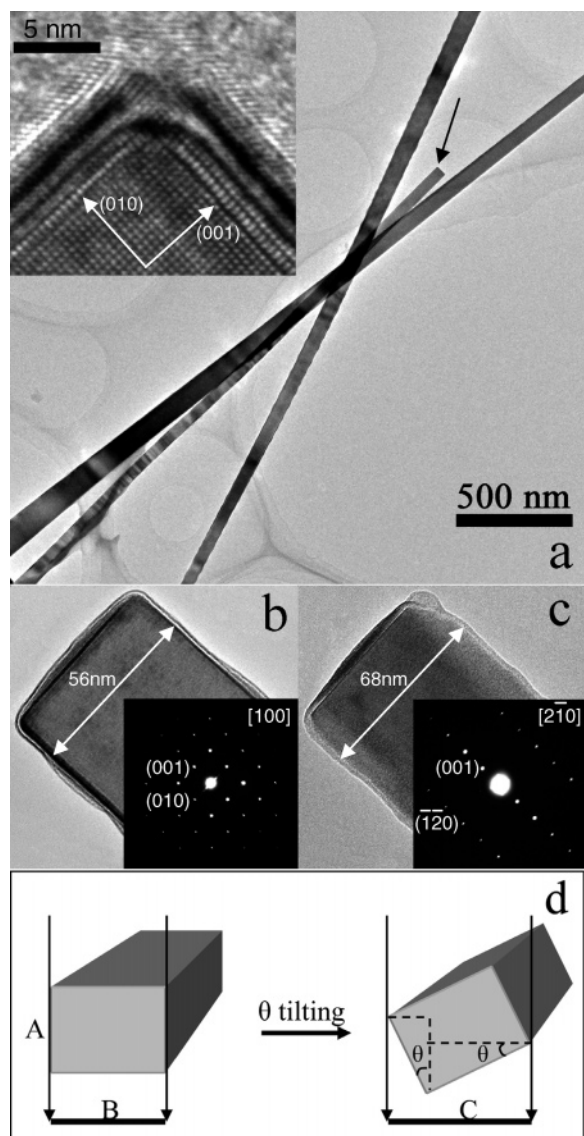


Figure 1. (a) TEM image of GdB₆ nanowires. Inset is a high-resolution lattice image of the tip's top-left corner of the nanowire marked by a dark arrow. (b–c) TEM images and selected area diffraction patterns taken from the same nanowire along its [100] and [210] lattice directions, respectively. (d) Illustration of the tilting process in reconstructing the morphology of the nanowire.

and the inset is an emission pattern recorded at an applied voltage of 750 V. The ring-like feature in the emission pattern is attributed to the fact that the local electric field was more enhanced at the edges and corners of the tip-top surface and therefore induced more emission from a circle of emission sites. We also performed a numerical simulation (FEMLAB) using a model based on the experimental conditions and obtained a local electric field enhancement factor $\beta = 3.3 \times 10^6 \text{ m}^{-1}$ at the edges of the top surface. By substituting β into the Fowler–Nordheim plot with slope $k = -1.02 \times 10^{38} \phi^{3/2}/\beta$, we obtained the value of work function for the GdB₆ nanowire to be about $1.53 \pm 0.2 \text{ eV}$, which agrees well with the reported value.² The lower work function of the GdB₆ can also be seen by directly comparing its emission current with that of a LaB₆ nanowire emitter. For example, at 750 V, the GdB₆ nanowire emitter produces more than 50 nA emission current, which is more than 5 times larger than the current drawn from the LaB₆ nanowire emitter working under same conditions.⁸

In conclusion, we have developed a CVD process that is able to produce GdB₆ nanowires of well characterized morphology. The

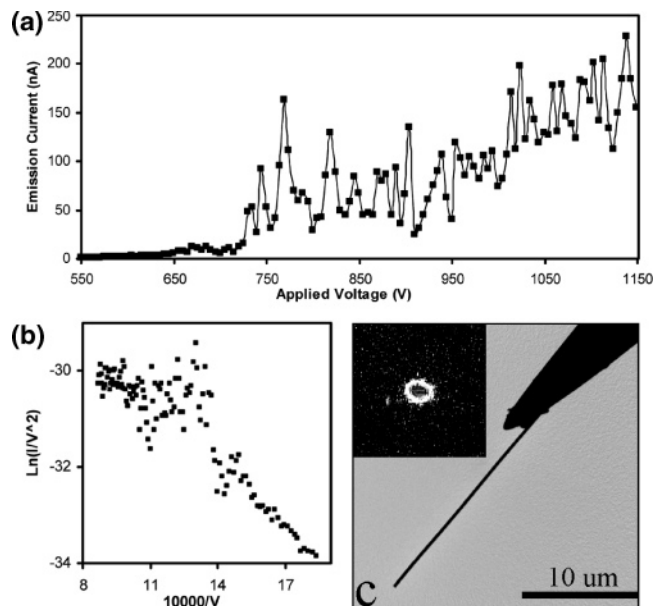


Figure 2. (a) Field emission I – V curve from a GdB₆ single nanowire. (b) Fowler–Nordheim plot of the field emission I – V curve. (c) Low-magnification TEM image of the single nanowire field emitter. Inset is the field emission pattern recorded on a phosphor screen.

nanowires have a rectangular cross-section with a width of about 50 nm and have a length extending to more than several microns. The growth direction of the nanowires is its $\langle 001 \rangle$ lattice direction, and they have flat tips and walls which are all terminated by the $\{100\}$ lattice planes. A GdB₆ single nanowire field emitter produced emission current of more than 150 nA at an average applied field under $3.2 \text{ V}/\mu\text{m}$. The work function of the GdB₆ nanowires was determined to be about 1.5 eV, which is lower than that of LaB₆ nanowire emitters. These GdB₆ nanowires have great potential use as point electron emitters for applications including providing point emission sources for TEM, SEM, flat panel displays, as well as other electronic devices that require high-performance electron sources.

Acknowledgment. We thank H. Jing and Dr. R. Superfine for assistance in the simulations and use of SEM, and Dr. J. Zhang for assistance in field emission measurement. J.T. is partially supported by the Japan–U.S. Collaborative Scientific Research Program of JSPS.

Supporting Information Available: SEM image, EDX spectrum, computer simulation, and procedure descriptions. This material is available free of charge via the Internet at <http://pubs.acs.org>.

References

- (1) Lafferty, J. M. *J. Appl. Phys.* **1951**, *22*, 299.
- (2) Kudintseva, G. A.; Kuznetsova, G. M.; Bondarenko, V. P.; Selivanova, N. F.; Shlyuko, V. Ya. *Poroshkovaya Metallurgiya* **1967**, *2*, 45.
- (3) Tanaka, T.; Nishitani, R.; Oshima, C.; Bannai, E.; Kawai, S. *J. Appl. Phys.* **1980**, *51*, 3877.
- (4) Storms, E. K.; Mueller, B. A. *J. Appl. Phys.* **1981**, *52*, 2966.
- (5) (a) Fowler, R. H.; Nordheim, L. *Proc. R. Soc. London* **1928**, *119*, 173. (b) Brodie, I.; Spindt, C. A. In *Advances in Electronics and Electron Physics*; Hawkes, P. W., Ed.; Academic Press: San Diego, 1992; Vol. 83, Chapter 2.
- (6) Jonge, N. D.; Allioux, M.; Oostveen, J. T.; Teo, K. B. K.; Milne, W. I. *Phys. Rev. Lett.* **2005**, *94*, 186807.
- (7) Zhang, H.; Zhang, Q.; Tang, J.; Qin, L.-C. *J. Am. Chem. Soc.* **2005**, *127*, 2862.
- (8) Zhang, H.; Zhang, Q.; Tang, J.; Qin, L.-C. *J. Am. Chem. Soc.* **2005**, *127*, 8002.
- (9) Zhang, H.; Zhang, Q.; Zhao, G.-P.; Yang, G.; Zhang, J.; Tang, J.; Zhou, O.; Qin, L.-C. *Adv. Mater.* **2005**, in press.

JA054251P